NASA Technical Paper 3368

September 1993

Room Temperature Degradation of $YBa_2Cu_3O_{7-x}$ Superconductors in Varying Relative Humidity Environments

M. W. Hooker, S. A. Wise,
I. A. Carlberg, R. M. Stephens,
R. T. Simchick, and A. Farjami

NASA Technical Paper 3368

1993

Room Temperature Degradation of $YBa_2Cu_3O_{7-x}$ Superconductors in Varying Relative Humidity Environments

M. W. Hooker
Clemson University
Clemson, South Carolina

S. A. Wise, I. A. Carlberg,
and R. M. Stephens
Langley Research Center
Hampton, Virginia

R. T. Simchick
Lockheed Engineering & Sciences Company
Hampton, Virginia

A. Farjami
Christopher Newport University
Newport News, Virginia

Abstract

An aging study was performed to determine the stability of $YBa_2Cu_3O_{7-x}$ ceramics in humid environments at 20°C. In this study, fired ceramic specimens were exposed to humidity levels ranging from 30.5 to 100 percent for 2-, 4-, and 6-week time intervals. After storage under these conditions, the specimens were characterized by X-ray diffraction (XRD), scanning electron microscopy (SEM), and electrical resistance measurements.

At every storage condition evaluated, the fired ceramics were found to interact with H_2O present in the surrounding environment, resulting in the decomposition of the $YBa_2Cu_3O_{7-x}$ phase. XRD data showed that $BaCO_3$, CuO, and Y_2BaCuO_5 were present after aging and that the peak intensities of these impurity phases increased both with increasing humidity level and with increasing time of exposure. Additionally, SEM analyses of the ceramic microstructures after aging revealed the development of needle-like crystallites along the surface of the test specimens after aging.

Furthermore, the superconducting transition temperature T_c was found to decrease both with increasing humidity level and with increasing time of exposure. All the specimens aged at 30.5, 66, and 81 percent relative humidity exhibited superconducting transitions above 80 K, although these values were reduced by the exposure to the test conditions. Conversely, the specimens stored in direct contact with water (100 percent relative humidity) exhibited no superconducting transitions.

Introduction

Since the discovery of the $YBa_2Cu_3O_{7-x}$ high-temperature superconductor compound (ref. 1), several difficulties have been encountered in manufacturing and storing these materials because of their chemical instability in the presence of water. The chemical instabilty of this superconducting phase both in high-humidity environments and in direct contact with water at temperatures ranging from 25° to 80°C has been the subject of several studies appearing in the technical literature (refs. 2–8).

In an X-ray diffraction study of the decomposition of the superconducting phase in water, Yan et al. (ref. 2) found that the $YBa_2Cu_3O_{7-x}$ superconducting phase decomposes into Y_2BaCuO_5, $BaCO_3$, and CuO when exposed to aqueous environments by the following two-stage reaction:

$$2YBa_2Cu_3O_{7-x} + 3H_2O \rightarrow Y_2BaCuO_5 + 3Ba(OH)_2 + 5CuO + \frac{1}{2}O_2 \quad (1)$$

and

$$Ba(OH)_2 + CO_2 \rightarrow BaCO_3 + H_2O \quad (2)$$

In this study, the $YBa_2Cu_3O_{7-x}$ phase was found to decompose upon direct contact with water at 25°C as well as upon exposure to high relative humidity levels at elevated temperatures (85°C at 85 percent relative humidity).

In another study, Fitch and Burdick (ref. 7) examined the microstructures of $YBa_2Cu_3O_{7-x}$ ceramics after 4 hr of exposure to 100 percent relative humidity at 80°C. They found that the percentage of superconducting phase present had been reduced by approximately 60 percent and that secondary phases had developed in the grain boundaries. These secondary phases were identified as $BaCO_3$ and Y_2BaCuO_5 by X-ray diffraction. Furthermore, SEM analyses of the microstructures of the corroded specimens revealed the development of needle-like crystals both on the surfaces of the grains and along the grain boundaries.

The decomposition of the superconducting phase by water is thought (refs. 2–8) to be due to the leaching of Ba from the ceramic to form $Ba(OH)_2$ along the surface of the ceramic. As $Ba(OH)_2$ is produced, Y_2BaCuO_5 and CuO are simultaneously formed as the decomposition reaction proceeds. Upon exposure to atmospheric conditions, the $Ba(OH)_2$ present on the surface of the test specimens is converted to $BaCO_3$ by the interaction of the hydrated phase with CO_2 present in the atmosphere, as described by reaction (2).

The decomposition of $YBa_2Cu_3O_{7-x}$ ceramics in the presence of water has been compared (ref. 6) with the dissolution of alkali silicate glasses and calcium silicate cements. In general, when these materials are exposed to water, a water-soluble element reacts with hydronium ions in the water to form a metal hydroxide (e.g., M(OH)) layer on the surface of the ceramic (refs. 9 and 10). Typically, these reactions take place along the grain boundaries in polycrystalline ceramics, and the reaction layer becomes thicker as the time of exposure increases (ref. 11).

In this report, the chemical stability of $YBa_2Cu_3O_{7-x}$ ceramics is evaluated at relative

humidity levels ranging from 30.5 to 100 percent for up to 6 weeks at 20°C to determine the effects of long-term storage on these materials. After exposure to the humid environments, the superconductive specimens were evaluated by Cu-$k\alpha$ X-ray diffraction, scanning electron microscopy, and standard dc four-probe resistance measurements to determine the effects of the exposure conditions on the superconducting materials.

Experimental Procedure

Synthesis of Y-Ba-Cu-O Superconductors

The $YBa_2Cu_3O_{7-x}$ compound used in this work was produced by the solid-state reaction of Y_2O_3, $BaCO_3$, and CuO in a manner similar to that described by Cava et al (ref. 12). In this process, stoichiometric blends of the precursor powders were ball milled for 30 min in deionized water. The powder was subsequently poured into a stainless steel pan, dried, pressed into loose compacts, and calcined for 8 hr at 900°C. Upon cooling, the compacts were crushed with a mortar and pestal, pressed, and calcined as before. This procedure was repeated a total of three times.

After the calcining treatments, the crushed powder was ball milled in acetone for 2 hr and dried. The test specimens for the aging experiments were prepared by pressing the milled powder into 2.5-cm-diameter disks at 7 MPa and firing to 950°C for 8 hr in air. The sintered disks were then annealed in flowing oxygen at 650°C for 15 hr to produce the superconducting phase.

The resulting disks were cut into rectangular specimens approximately 0.2 cm thick with a diamond saw. Some of these specimens were characterized prior to aging by using Cu-$k\alpha$ X-ray diffraction, dc four-probe resistance measurements, and scanning electron microscopy to ensure phase purity in the as-produced ceramics.

Exposure to Humid Environments

Once produced, the $YBa_2Cu_3O_{7-x}$ specimens were stored in sealed containers with controlled humidity levels. Constant relative humidities of 30.5, 66, and 81 percent were produced by placing solutions with excess amounts of NaCl, $NaNO_2$, and $(NH_4)_2SO_4$, respectively, in sealed desiccators (ref. 13). To determine the effects of 100 percent relative humidity, $YBa_2Cu_3O_{7-x}$ specimens were stored in deionized water during the test period. Superconductive specimens were placed in the four constant-humidity chambers for 2-, 4-, and 6-week periods to determine the effects of exposure to the humid environments over time.

Characterization of Aged Specimens

After aging at the controlled humidity levels, the specimens were characterized by Cu-$k\alpha$ X-ray diffraction (XRD) to identify any secondary phases that may have been produced during the exposure period. Particular emphasis was placed on the presence of $BaCO_3$ in the diffraction patterns, as Ba is the most likely of the three metal ions in the superconductive compound to react with the humid environment. Scanning electron microscopy (SEM) analyses were also performed on the specimens after aging to determine the effects of the various storage conditions on the microstructure.

Additionally, dc four-probe resistance measurements were performed on each ceramic specimen after aging to identify any degradation of the superconducting transition temperature T_c. In these analyses, particular attention was given not only to the value of T_c, but to the width of the superconducting transition, as wide transitions are often observed for superconducting materials with impurity phases present.

Experimental Results

Synthesis of Y-Ba-Cu-O Superconductors

The solid-state synthesis technique employed resulted in the formation of phase-pure superconductive materials as demonstrated by X-ray diffraction and dc four-probe measurement results. The XRD pattern obtained for the as-produced ceramics was in agreement with those reported in the technical literature (ref. 12). Furthermore, the resistance measurements show that the specimens possess sharp superconductive transitions above 90 K ($T_{c,\text{zero}} = 91$ K).

The SEM analyses of the as-produced specimens show that the $YBa_2Cu_3O_{7-x}$ ceramics possess randomly oriented, rectangular grains typically observed for this compound (ref. 14). An XRD pattern, a resistance-versus-temperature plot, and an SEM micrograph for the as-produced materials are shown in figures 1 to 3, respectively.

XRD Analyses of Aged Specimens

The XRD analyses of the superconducting ceramic specimens stored at a constant relative humidity of 30.5 percent indicate that after 2 weeks of exposure, small quantities of $BaCO_3$ were present. In this instance, the most intense peak attributable to the presence of $BaCO_3$ (at diffraction angle

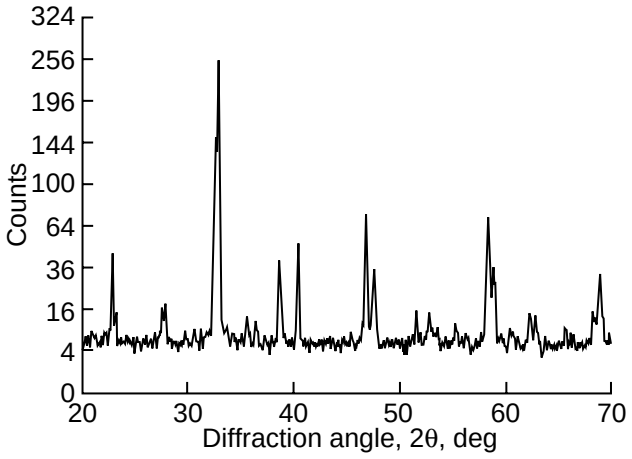

Figure 1. XRD pattern of $YBa_2Cu_3O_{7-x}$ produced by solid-state synthesis technique.

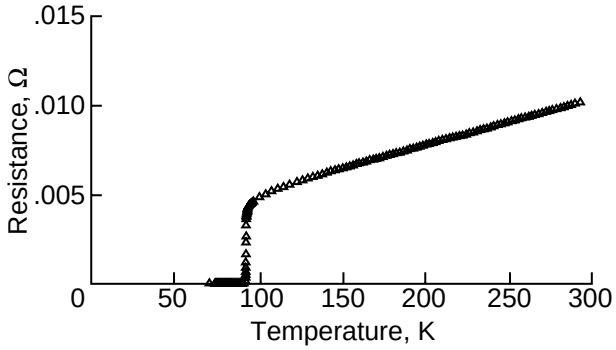

Figure 2. Resistance-versus-temperature plot of as-produced $YBa_2Cu_3O_{7-x}$.

Figure 3. SEM micrograph showing the rectangular grain structure of as-produced $YBa_2Cu_3O_{7-x}$ ceramics.

$2\theta = 23.9°$) was 2.5 percent that of the most intense $YBa_2Cu_3O_{7-x}$ peak ($2\theta = 32.4°$). The intensity of this peak was found to increase as the exposure time to this humidity level increased. After 4 weeks of exposure, the peak intensity was 5.8 percent of the largest $YBa_2Cu_3O_{7-x}$ peak, and after 6 weeks it was 6.5 percent of the largest $YBa_2Cu_3O_{7-x}$ peak.

Similar XRD patterns were obtained for the specimens aged at 66 and 81 percent relative humidity. At these two humidity levels, the peak intensity of the $BaCO_3$ peak was also found to increase with respect to that of the most intense $YBa_2Cu_3O_{7-x}$ peak as the exposure time was increased. The largest values for the ratios of the most intense $BaCO_3$ peak to that of the most intense $YBa_2Cu_3O_{7-x}$ peak (I/I_o) were 17 percent for the specimens stored at 66 percent relative humidity for 6 weeks and 20 percent for the specimens stored at 81 percent relative humidity for 6 weeks.

In addition to the formation of $BaCO_3$, peaks attributable to the presence of Y_2BaCuO_5 and CuO were identified on the surface of the specimens aged longer than 4 weeks at 66 percent relative humidity and longer than 2 weeks at 81 percent relative humidity. The relative peak intensities for these compounds were less than those attributable to $BaCO_3$, although the intensities of these peaks also increased as the time of exposure to the humid environment increased.

The specimens stored in direct contact with deionized water (100 percent relative humidity) were found to possess larger quantities of $BaCO_3$ than those stored at lower humidity levels. After 2 weeks of exposure to deionized water, the value of I/I_o was found to be 18 percent. This value was found to increase to 23 percent after 4 weeks, and after 6 weeks of exposure, the most intense peak observed in the XRD pattern was that of $BaCO_3$ ($I/I_o = 100$ percent). In this case, peaks for Y_2BaCuO_5 and CuO were also identified. The various phases identified in the XRD analyses are given in table 1. Furthermore, the relative peak intensities I/I_o for each of the experimental conditions are plotted against the time of exposure in figure 4. The XRD data for each experimental condition are provided in appendix A.

SEM Analyses of Aged Specimens

The SEM analyses of the samples aged at various humidity levels show the loss of the superconductive microstructure (see fig. 3) and the growth of small,

Table 1. Secondary Phases Identified by XRD Analysis and Their Relative Peak Intensities After Exposure to Various Humidity Levels

Relative humidity, percent	Exposure time, weeks	Secondary phases identified	Peak intensities I/I_o percent
30.5	2	$BaCO_3$	2
30.5	4	$BaCO_3$	5.6
30.5	6	$BaCO_3$	6.5
66	2	$BaCO_3$	10
66	4	$BaCO_3Y_2BaCuO_5$	11
66	6	$BaCO_3Y_2BaCuO_5$	13.5
81	2	$BaCO_3CuO$, Y_2BaCuO_5	11.5
81	4	$BaCO_3CuO$, Y_2BaCuO_5	16.7
81	6	$BaCO_3CuO$, Y_2BaCuO_5	20
100	2	$BaCO_3CuO$, Y_2BaCuO_5	15
100	4	$BaCO_3CuO$, Y_2BaCuO_5	25
100	6	$BaCO_3CuO$, Y_2BaCuO_5	100

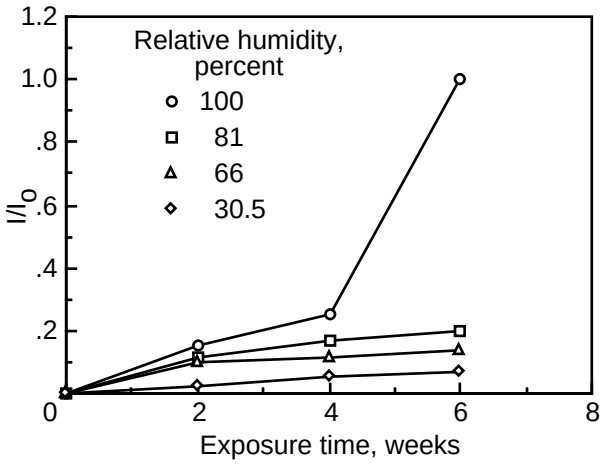

Figure 4. Relative peak intensities I/I_o for superconducting specimens stored under various relative humidity levels.

needle-like crystallites, presumably $BaCO_3$, on the surfaces of the aged specimens. The formation of these crystallites on the surface of a $YBa_2Cu_3O_{7-x}$ specimen stored at 66 percent relative humidity for 6 weeks is shown in figure 5. In this micrograph, the degradation of the surface of the ceramic is shown. Similar microstructures were also observed for specimens aged at relative humidity levels between 30.5 and 81 percent.

L-93-20

Figure 5. SEM micrograph showing formation of small, needle-like grains (bottom right) on surface of $YBa_2Cu_3O_{7-x}$ specimen stored at 66 percent relative humidity for 6 weeks.

The specimens stored in direct contact with water decomposed much faster than those stored at lower humidity levels. The more pronounced growth of these crystallites is shown in figure 6, in which the presence of 1–2-μm crystallites along the surface of the test specimen is observed.

L-93-21

Figure 6. SEM micrograph showing formation of $BaCO_3$ crystallites on surface of $YBa_2Cu_3O_{7-x}$ specimen stored at 100 percent relative humidity for 2 weeks (magnified 3000 times).

As the time of exposure to the 100 percent relative humidity was increased, the size of the crystals observed on the surface of the specimens also increased. The continued growth of the crystallites is shown in figures 7 and 8 for specimens aged in deionized water for 4 and 6 weeks, respectively. The microstructures shown in figures 6 through 8 are similar to those reported by Bansal and Sandkuhl (ref. 4), who studied the effects of exposure to high humidity levels (85–100 percent) at temperatures ranging from 25° to 55°C.

L-93-22

Figure 7. SEM micrograph illustrating continued growth of $BaCO_3$ crystallites on $YBa_2Cu_3O_{7-x}$ specimen stored at 100 percent relative humidity for 4 weeks.

L-93-23

Figure 8. SEM micrograph of decomposition products along surface of $YBa_2Cu_3O_{7-x}$ specimen stored at 100 percent relative humidity for 6 weeks.

Results of dc Four-Probe Resistance Measurements

Like the XRD results, the resistance measurements show that the exposure to each of the experimental conditions resulted in degradation of the superconducting specimen. At each relative humidity level tested, both the temperature of the onset of superconductivity ($T_{c,\text{onset}}$) and the temperature at which zero resistance is obtained ($T_{c,\text{zero}}$) were reduced after several weeks of exposure to the humid environments. (See table 2.)

Table 2. Values $T_{c,\text{onset}}$ and $T_{c,\text{zero}}$ for $YBa_2Cu_3O_{7-x}$ Specimens Stored in Humid Environments

Relative humidity, percent	Exposure time, weeks	$T_{c,\text{onset}}$	$T_{c,\text{zero}}$
30.5	2	92	88
30.5	4	91	87.5
30.5	6	89	86.5
66	2	92	87.5
66	4	92	88.5
66	6	91.5	87
81	2	91	87
81	4	88.5	85
81	6	86	82
100	2		
100	4		
100	6		

The superconducting transition temperature of the specimen stored at 30.5 percent relative humidity for 2 weeks decreased from 91 to 88 K, although the temperature of the onset of superconductivity was unchanged. After 4 weeks of exposure at 30.5 percent relative humidity, the values for $T_{c,\text{onset}}$ and $T_{c,\text{zero}}$ were decreased to 91 and 87.5 K, respectively. After 6 weeks of exposure at this humidity level, the values of $T_{c,\text{onset}}$ and $T_{c,\text{zero}}$ were further decreased to 89 and 86.5 K. Resistance-versus-temperature plots for the specimens aged at 30.5 percent relative humidity are shown in figure 9.

The resistance-versus-temperature plots for the specimens stored at 66 and 81 percent relative humidity were similar to those of the ceramics stored at 30.5 percent. In each instance, the values for

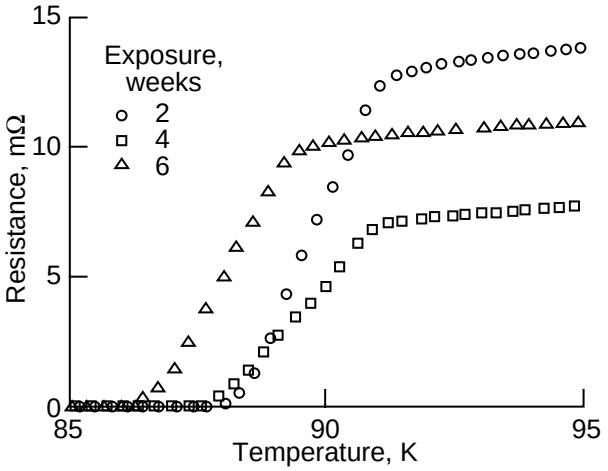

Figure 9. Resistance-versus-temperature plot of superconducting specimens aged at 30.5 percent relative humidity.

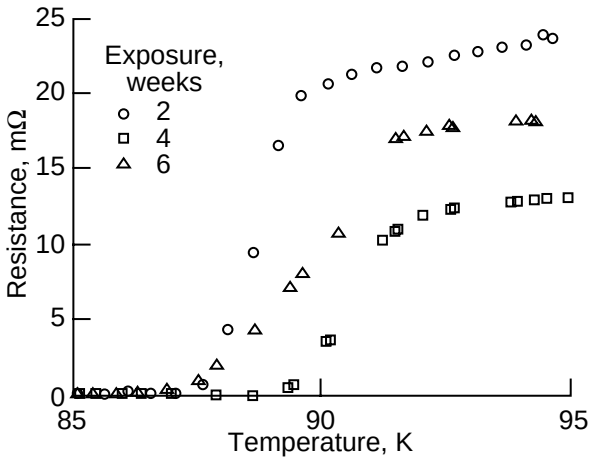

Figure 10. Resistance-versus-temperature plot of superconducting specimens aged at 66 percent relative humidity.

$T_{c,\text{onset}}$ and $T_{c,\text{zero}}$ were reduced from the values of the as-produced material. The resistance-versus-temperature data obtained for these specimens are shown in figures 10 and 11.

None of the specimens aged in direct contact with water (100 percent relative humidity) were found to exhibit a superconducting transition. This result was anticipated from the XRD studies, which show that these specimens are composed primarily of decomposition products.

Discussion

The interaction of $YBa_2Cu_3O_{7-x}$ with water present in the sealed containers resulted in the chemical decomposition of the superconductive material and an associated reduction of the superconducting transition temperature T_c of the test specimens at every humidity level tested. After 2 weeks of exposure at 30.5 percent relative humidity, the presence of $BaCO_3$ was detected on the surface of the specimen by X-ray diffraction. Although the SEM analyses showed little degradation of the microstructure, the resistance-versus-temperature measurements show that $T_{c,\text{zero}}$ was reduced from 91 to 88 K. These results indicate that exposure to ambient conditions for relatively short periods of time may adversely affect the properties of the ceramic. Furthermore, these results indicate that exposure to low humidity levels can cause degradation at room temperature, affecting long-term storage of the materials.

As the time of exposure and the humidity level increased, the ceramics reacted more vigorously with

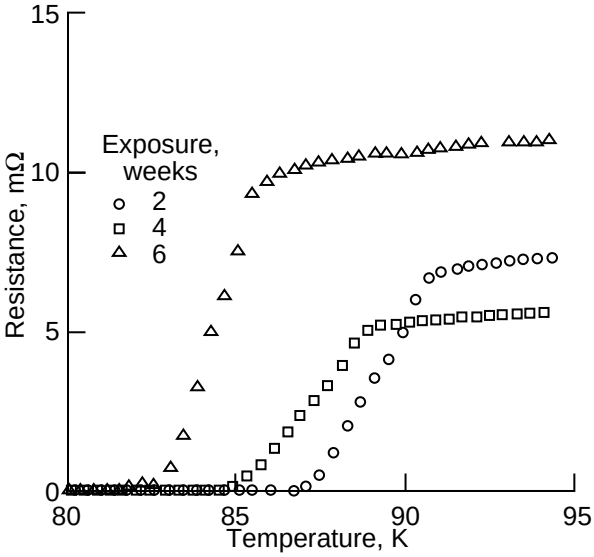

Figure 11. Resistance-versus-temperature plot of superconducting specimens aged at 81 percent relative humidity.

the water vapor present to form $BaCO_3$ on the surface of the superconductor, as described by Yan et al. (ref. 2). As this decomposition results in the deposition of impurity phases (e.g., Y_2BaCuO_5 and $BaCO_3$) along the grain boundaries of the ceramic, the electrical properties of the material will decline (ref. 7). The decrease in the electrical properties is attributable to the presence of these impurity phases in the grain boundaries (ref. 15), which are already considered to be electrical "weak links" in the superconducting ceramic (ref. 16).

The relationship between the degradation of the superconductive transition temperature with increasing impurity phase concentrations may be best illustrated by plotting the relative peak intensity of the largest $BaCO_3$ peaks (I/I_o) from the XRD evaluation versus the corresponding $T_{c,\text{zero}}$ values of the ceramics stored between 30.5 and 81 percent relative humidity, as shown in figure 12. In this graph, the humidity level at which the specimens were stored is not taken into account. Nevertheless, the graph indicates that the reduction of the superconducting transition temperature is a function of the impurity phase concentration.

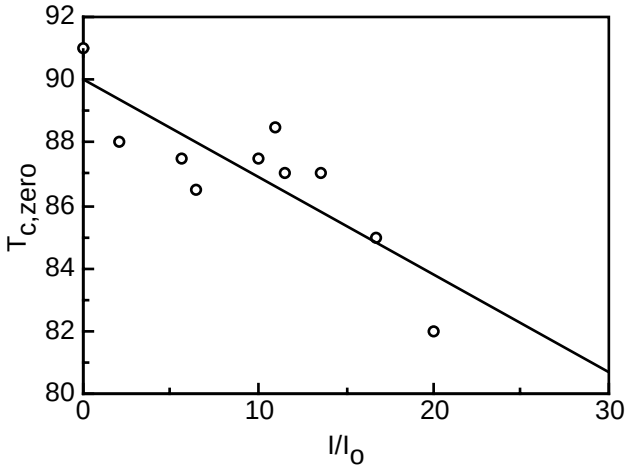

Figure 12. Relationship between $T_{c,\text{zero}}$ and relative peak intensity I/I_o for barium carbonate present in test specimens stored at 30.5, 66, and 81 percent relative humidity.

In each of the experiments, the XRD and dc four-probe resistance measurements show a decreasing superconducting transition temperature with increasing $BaCO_3$ peak intensity (I/I_o). This correlation was not observed for the specimens immersed in water, as shown in figure 4. For example, the XRD results obtained for specimens immersed in water for 2 weeks show that the value of I/I_o is 15 percent, which is similar to that for specimens stored at other conditions (e.g., $I/I_o = 16.7$ percent for specimens stored at 81 percent relative humidity for 4 weeks). However, no evidence of superconductivity was found in these specimens by dc four-probe analysis.

This combination of results indicates that the reactive nature of the liquid/solid and vapor/solid interfaces is different. The interaction along the vapor/solid interface results in the direct deposition of $BaCO_3$ along the surface of the test specimens. Conversely, the leaching of Ba from the $YBa_2Cu_3O_{7-x}$ ceramics results in both $BaCO_3$ produced on the surface and Ba ions lost in solution, which are not accounted for in the XRD results. Thus, in the previously mentioned example, superconductivity is lost altogether, although the XRD results show $BaCO_3$ levels indicative of a specimen that should possess a superconducting transition.

Concluding Remarks

The combined results show that H_2O present in the atmosphere at 20°C reacts with the $YBa_2Cu_3O_{7-x}$ compound to form $BaCO_3$, CuO, and Y_2BaCuO_5 on the surface of the ceramics, as previously described in the technical literature.

In this study, reduction of the superconducting transition temperature was found to correlate with the presence of $BaCO_3$ and other impurity phases on the surface of the ceramic. The presence of these impurity phases on the surface of the test specimens was identified by X-ray diffraction and SEM analyses. The decrease in the superconductive transition temperature is due to the deposition of insulating decomposition products along the grain boundaries, further reducing intergranular connectivity.

The significant result of this study is that these interactions take place at such low relative humidity and temperature combinations that storage of superconductive devices may be a key issue in the use of these materials. To combat the reactivity of this superconductive compound with ambient moisture, protective overcoats may be required to avoid any degradation of the ceramics during both storage and operation.

NASA Langley Research Center
Hampton, VA 23681-0001
July 1, 1993

Appendix A

X-Ray Diffraction Data

The XRD data presented in this appendix in tables A1–A13 are displayed in terms of the diffraction angle 2θ, the relative peak intensity, and the phase identified by a peak occurring at this angle. The relative intensity term I/I_o is calculated by dividing the intensity of a peak by the intensity of the largest peak observed in the diffraction pattern.

Table A1. XRD Data for As-Produced $YBa_2Cu_3O_{7-x}$

Diffraction angle, 2θ, deg	I/I_o	Phase identified
22.8	10	$YBa_2Cu_3O_{7-x}$
32.7	100	$YBa_2Cu_3O_{7-x}$
38.6	15	$YBa_2Cu_3O_{7-x}$
40.4	20	$YBa_2Cu_3O_{7-x}$
46.8	35	$YBa_2Cu_3O_{7-x}$
47.5	20	$YBa_2Cu_3O_{7-x}$
58.4	40	$YBa_2Cu_3O_{7-x}$
58.8	25	$YBa_2Cu_3O_{7-x}$
68.8	25	$YBa_2Cu_3O_{7-x}$

Table A2. XRD Data for $YBa_2Cu_3O_{7-x}$ Stored at 30.5 Percent Relative Humidity for 2 Weeks

Diffraction angle, 2θ, deg	I/I_o	Phase identified
22.8	9	$YBa_2Cu_3O_{7-x}$
23.9	2.5	$BaCO_3$
32.7	100	$YBa_2Cu_3O_{7-x}$
38.6	10	$YBa_2Cu_3O_{7-x}$
40.4	19	$YBa_2Cu_3O_{7-x}$
46.8	34	$YBa_2Cu_3O_{7-x}$
47.5	20	$YBa_2Cu_3O_{7-x}$
58.4	38	$YBa_2Cu_3O_{7-x}$
58.8	27	$YBa_2Cu_3O_{7-x}$
68.8	22	$YBa_2Cu_3O_{7-x}$

Table A3. XRD Data for $YBa_2Cu_3O_{7-x}$ Stored at 30.5 Percent Relative Humidity for 4 Weeks

Diffraction angle, 2θ, deg	I/I_o	Phase identified
22.8	8	$YBa_2Cu_3O_{7-x}$
23.9	5.8	$BaCO_3$
32.7	100	$YBa_2Cu_3O_{7-x}$
38.6	13	$YBa_2Cu_3O_{7-x}$
40.4	22	$YBa_2Cu_3O_{7-x}$
46.8	33	$YBa_2Cu_3O_{7-x}$
47.5	18	$YBa_2Cu_3O_{7-x}$
58.4	45	$YBa_2Cu_3O_{7-x}$
58.8	27	$YBa_2Cu_3O_{7-x}$
68.8	24	$YBa_2Cu_3O_{7-x}$

Table A4. XRD Data for $YBa_2Cu_3O_{7-x}$ Stored at 30.5 Percent Relative Humidity for 6 Weeks

Diffraction angle, 2θ, deg	I/I_o	Phase identified
22.8	6	$YBa_2Cu_3O_{7-x}$
23.9	6.5	$BaCO_3$
27.9	5.8	$BaCO_3$
29.4	4.5	Y_2BaCuO_5
32.7	100	$YBa_2Cu_3O_{7-x}$
38.6	13	$YBa_2Cu_3O_{7-x}$
40.4	19	$YBa_2Cu_3O_{7-x}$
46.8	30	$YBa_2Cu_3O_{7-x}$
47.5	17	$YBa_2Cu_3O_{7-x}$
52.6	5	$BaCO_3$
53.2	4	$BaCO_3$
55.2	6	$BaCO_3$
58.4	43	$YBa_2Cu_3O_{7-x}$
58.8	27	$YBa_2Cu_3O_{7-x}$
68.8	24	$YBa_2Cu_3O_{7-x}$

Table A5. XRD Data for $YBa_2Cu_3O_{7-x}$ Stored at 66 Percent Relative Humidity for 2 Weeks

Diffraction angle, 2θ, deg	I/I_o	Phase identified
22.8	9	$YBa_2Cu_3O_{7-x}$
23.9	10	$BaCO_3$
32.7	100	$YBa_2Cu_3O_{7-x}$
38.6	14	$YBa_2Cu_3O_{7-x}$
40.4	20	$YBa_2Cu_3O_{7-x}$
46.8	35	$YBa_2Cu_3O_{7-x}$
47.5	22	$YBa_2Cu_3O_{7-x}$
58.4	43	$YBa_2Cu_3O_{7-x}$
58.8	25	$YBa_2Cu_3O_{7-x}$
68.8	24	$YBa_2Cu_3O_{7-x}$

Table A6. XRD Data for $YBa_2Cu_3O_{7-x}$ Stored at 66 Percent Relative Humidity for 4 Weeks

Diffraction angle, 2θ, deg	I/I_o	Phase identified
22.8	9	$YBa_2Cu_3O_{7-x}$
23.9	11	$BaCO_3$
27.7	6.5	$BaCO_3$
29.4	4.5	Y_2BaCuO_5
32.7	100	$YBa_2Cu_3O_{7-x}$
38.6	15	$YBa_2Cu_3O_{7-x}$
40.4	16	$YBa_2Cu_3O_{7-x}$
46.8	28	$YBa_2Cu_3O_{7-x}$
47.5	20	$YBa_2Cu_3O_{7-x}$
52.5	8	$BaCO_3$
58.4	56	$YBa_2Cu_3O_{7-x}$
58.8	30	$YBa_2Cu_3O_{7-x}$
68.8	27	$YBa_2Cu_3O_{7-x}$

Table A7. XRD Data for $YBa_2Cu_3O_{7-x}$ Stored at 66 Percent Relative Humidity for 6 Weeks

Diffraction angle, 2θ, deg	I/I_o	Phase identified
22.8	7	$YBa_2Cu_3O_{7-x}$
23.9	13.5	$BaCO_3$
28.1	7.5	$BaCO_3$
29.7	5	Y_2BaCuO_5
32.7	100	$YBa_2Cu_3O_{7-x}$
38.6	18	$YBa_2Cu_3O_{7-x}$
40.4	18	$YBa_2Cu_3O_{7-x}$
46.8	36	$YBa_2Cu_3O_{7-x}$
47.5	16	$YBa_2Cu_3O_{7-x}$
51.7	9	$YBa_2Cu_3O_{7-x}$
53.3	7	$BaCO_3$
58.4	47	$YBa_2Cu_3O_{7-x}$
58.8	27	$YBa_2Cu_3O_{7-x}$
68.8	26	$YBa_2Cu_3O_{7-x}$

Table A8. XRD Data for $YBa_2Cu_3O_{7-x}$ Stored at 81 Percent Relative Humidity for 2 Weeks

Diffraction angle, 2θ, deg	I/I_o	Phase identified
22.8	9	$YBa_2Cu_3O_{7-x}$
23.9	11.5	$BaCO_3$
28.1	7.5	$BaCO_3$
30.0	5	Y_2BaCuO_5
32.7	100	$YBa_2Cu_3O_{7-x}$
36.0	6	$BaCO_3$
36.6	6	CuO
38.6	14	$YBa_2Cu_3O_{7-x}$
40.4	20	$YBa_2Cu_3O_{7-x}$
46.8	36	$YBa_2Cu_3O_{7-x}$
47.5	16	$YBa_2Cu_3O_{7-x}$
53.3	9	$BaCO_3$
58.4	47	$YBa_2Cu_3O_{7-x}$
58.8	27	$YBa_2Cu_3O_{7-x}$
68.8	26	$YBa_2Cu_3O_{7-x}$

Table A9. XRD Data for $YBa_2Cu_3O_{7-x}$ Stored at 81 Percent Relative Humidity for 4 Weeks

Diffraction angle, 2θ, deg	I/I_o	Phase identified
22.8	9	$YBa_2Cu_3O_{7-x}$
23.9	16.7	$BaCO_3$
28.1	7	$BaCO_3$
29.7	7	Y_2BaCuO_5
32.7	100	$YBa_2Cu_3O_{7-x}$
36.7	6	CuO
38.6	18	$YBa_2Cu_3O_{7-x}$
40.4	21	$YBa_2Cu_3O_{7-x}$
46.8	37	$YBa_2Cu_3O_{7-x}$
47.5	21	$YBa_2Cu_3O_{7-x}$
51.7	7	$YBa_2Cu_3O_{7-x}$
53.3	9	$BaCO_3$
55.4	6	$BaCO_3$
58.4	43	$YBa_2Cu_3O_{7-x}$
58.8	25	$YBa_2Cu_3O_{7-x}$
68.8	26	$YBa_2Cu_3O_{7-x}$

Table A10. XRD Data for $YBa_2Cu_3O_{7-x}$ Stored at 81 Percent Relative Humidity for 6 Weeks

Diffraction angle, 2θ, deg	I/I_o	Phase identified
22.8	9	$YBa_2Cu_3O_{7-x}$
23.9	20	$BaCO_3$
28.1	8	$BaCO_3$
29.9	9	Y_2BaCuO_5
32.7	100	$YBa_2Cu_3O_{7-x}$
36.7	10	CuO
38.6	14	$YBa_2Cu_3O_{7-x}$
40.4	20	$YBa_2Cu_3O_{7-x}$
46.8	35	$YBa_2Cu_3O_{7-x}$
47.5	22	$YBa_2Cu_3O_{7-x}$
51.7	8	$YBa_2Cu_3O_{7-x}$
53.3	10	$BaCO_3$
55.4	8	$BaCO_3$
58.4	43	$YBa_2Cu_3O_{7-x}$
58.8	25	$YBa_2Cu_3O_{7-x}$
68.8	24	$YBa_2Cu_3O_{7-x}$

Table A11. XRD Data for $YBa_2Cu_3O_{7-x}$ Stored at 100 Percent Relative Humidity for 2 Weeks

Diffraction angle, 2θ, deg	I/I_o	Phase identified
22.8	8	$YBa_2Cu_3O_{7-x}$
23.9	15	$BaCO_3$
27.8	7	$BaCO_3$
29.5	8.5	Y_2BaCuO_5
32.7	100	$YBa_2Cu_3O_{7-x}$
35.4	14	CuO
38.6	24	$YBa_2Cu_3O_{7-x}$
40.4	17	$YBa_2Cu_3O_{7-x}$
46.8	31	$YBa_2Cu_3O_{7-x}$
47.5	15	$YBa_2Cu_3O_{7-x}$
51.7	8	$YBa_2Cu_3O_{7-x}$
53.0	6	$BaCO_3$
58.4	52	$YBa_2Cu_3O_{7-x}$
58.8	28	$YBa_2Cu_3O_{7-x}$
68.8	25	$YBa_2Cu_3O_{7-x}$

Table A12. XRD Data for $YBa_2Cu_3O_{7-x}$ Stored at 100 Percent Relative Humidity for 4 Weeks

Diffraction angle, 2θ, deg	I/I_o	Phase identified
22.8	9	$YBa_2Cu_3O_{7-x}$
23.9	25	$BaCO_3$
27.9	7.5	$BaCO_3$
29.8	5.4	Y_2BaCuO_5
32.7	100	$YBa_2Cu_3O_{7-x}$
34.8	4	$BaCO_3$
36.0	10	CuO
38.6	19	CuO, $YBa_2Cu_3O_{7-x}$
44.4	17	$YBa_2Cu_3O_{7-x}$
45.3	10	$BaCO_3$
46.8	35	$YBa_2Cu_3O_{7-x}$
47.5	14	$YBa_2Cu_3O_{7-x}$
49.0	6	$BaCO_3$
58.4	61	$YBa_2Cu_3O_{7-x}$
58.8	33	$YBa_2Cu_3O_{7-x}$
68.8	28	$YBa_2Cu_3O_{7-x}$

Table A13. XRD Data for $YBa_2Cu_3O_{7-x}$ Stored at 100 Percent Relative Humidity for 6 Weeks

Diffraction angle, 2θ, deg	I/I_o	Phase identified
22.8	13	$YBa_2Cu_3O_{7-x}$
23.9	100	$BaCO_3$
27.9	36.5	$BaCO_3$
30.0	10	Y_2BaCuO_5
32.7	16	$YBa_2Cu_3O_{7-x}$
33.9	65	$BaCO_3$
34.8	4	$BaCO_3$
35.6	22	CuO
38.6	41	CuO, $YBa_2Cu_3O_{7-x}$
42.0	30	$BaCO_3$
42.9	16	$BaCO_3$
44.4	27	$BaCO_3$
46.8	68	$YBa_2Cu_3O_{7-x}$
47.4	26	$YBa_2Cu_3O_{7-x}$
49.0	17	$BaCO_3$
56.0	24	$BaCO_3$
58.4	43	$YBa_2Cu_3O_{7-x}$
58.3	30	$YBa_2Cu_3O_{7-x}$
58.8	22	$YBa_2Cu_3O_{7-x}$
61.0	30	CuO
61.2	32	CuO
62.1	17	CuO
68.8	24	$YBa_2Cu_3O_{7-x}$

References

1. Wu, M. K.; Ashburn, J. R.; Torng, C. J.; Hor, P. H.; and Meng, R. L.: Superconductivity at 93 K in a New Mixed-Phase Y-Ba-Cu-O Compound System at Ambient Pressure. *Phys. Review Lett.*, vol. 58, Mar. 2, 1987, pp. 908–910.

2. Yan, M. F.; Barns, R. L.; O'Bryan, H. M., Jr.; Gallagher, P. K.; and Sherwood, R. C.: Water Interaction With the Superconducting YBa2Cu3O7 Phase. *Appl. Phys. Lett.*, vol. 51, Aug. 17, 1987, pp. 532–534.

3. Barns, R. L.; and Laudise, R. A.: Stability of Superconducting YBa2Cu3O7 in the Presence of Water. *Appl. Phys. Lett.*, vol. 51, Oct. 26, 1987, pp. 1373–1375.

4. Bansal, Narottam P.; and Sandkuhl, Ann L.: Chemical Durability of High-Temperature Superconductor YBa2Cu3O(7-x) in Aqueous Environments. *Appl. Phys. Lett.*, vol. 52, Jan. 25, 1988, pp. 323–325.

5. Garland, M. M.: Fabrication of the BilSrlCalCu2O(x) High T(c) Superconductor. *Appl. Phys. Lett.*, vol. 52, May 30, 1988, pp. 1913, 1914.

6. Trolier, Susan E.; Atkinson, Scott D.; Fuierer, Paul A.; Adair, James H.; and Newnham, Robert E.: Dissolution of $YBa_2Cu_3O_{(7-x)}$ in Various Solvents. *American Ceram. Soc. Bull.*, vol. 67, no. 4, 1988, pp. 759–762.

7. Fitch, Lawrence D.; and Burdick, Vernon L.: Water Corrosion of $YBa_2Cu_3O_{7-\delta}$ Superconductors. *J. American Ceram. Soc.*, vol. 72, no. 10, 1989, pp. 2020–2023.

8. Yokota, Katsuhiro; Kura, Takeshi; Ochi, Mitsukazu; and Katayama, Saichi: A Pathway for the Decomposition of $YBa_2Cu_3O_{7-x}$ in Water. *J. Mater. Res.*, vol. 5, no. 12, Dec. 1990, pp. 2790–2796.

9. Paul, A.: Chemical Durability of Glasses; a Thermodynamic Approach. *J. Mater. Sci.*, vol. 12, 1977, pp. 2246–2268.

10. Clark, A. E., Jr.; Pantano, C. G., Jr.; and Hench, L. L.: Auger Spectroscopic Analysis of Bioglass Corrosion Films. *J. American Ceram. Soc.*, vol. 59, Jan.–Feb. 1976, pp. 37–39.

11. Kingery, W. D.; Bowen, H. K.; and Uhlmann, D. R.: *Introduction to Ceramics*, Second ed. John Wiley & Sons, Inc., c.1960.

12. Cava, R. J.; Batlogg, B.; Van Dover, R. B.; Murphy, D. W.; and Sunshine, S.: Bulk Superconductivity at 91 K in Single-Phase Oxygen-Deficient Perovskite Ba2YCu30(9-delta). *Phys. Review Lett.*, vol. 58, Apr. 20, 1987, pp. 1676–1679.

13. Weast, Robert C., ed.: *CRC Handbook of Chemistry and Physics*, 66th ed. CRC Press, Inc., c.1985.

14. Alford, N. McN.; Button, T. W.; and Birchall, J. D.: Processing, Properties and Devices in High-T_c Superconductors. *Supercond. Sci. & Technol.*, vol. 3, 1990, pp. 1–7.

15. Kitazawa, K.; Kishio, K.; Hasegawa, T.; Ohtomo, A.; and Yaegashi, S.: Materials Aspects of Oxide Superconductors—Effect of Ambient Water on Superconductivity. *Proceedings of the Symposium on High-Temperature Superconductors*, Volume 99, Merwyn B. Brodsky, Robert C. Dynes, Koichi Kitazawa, and Harry L. Tuller, eds., Materials Research Soc., 1988, pp. 33–40.

16. Larbalestier, D. C.; Babcock, S. E.; Cai, X.; Daeumling, M.; Hampshire, D. P.; Kelly, T. F.; Lavanier, L. A.; Lee, P. J.; and Seuntjens, J.: Weak Links and the Poor Transport Critical Currents of the 123 Compounds. *Physica C*, vols. 153–155, 1988, pp. 1580–1585.

REPORT DOCUMENTATION PAGE

Form Approved
OMB No. 0704-0188

1. AGENCY USE ONLY *(Leave blank)*	2. REPORT DATE	3. REPORT TYPE AND DATES COVERED
	September 1993	Technical Paper

4. TITLE AND SUBTITLE
Room Temperature Degradation of $YBa_2Cu_3O_{7-x}$ Superconductors in Varying Relative Humidity Environments

5. FUNDING NUMBERS
WU 142-20-14-02

6. AUTHOR(S)
M. W. Hooker, S. A. Wise, I. A. Carlberg, R. M. Stephens, R. T. Simchick, and A. Farjami

7. PERFORMING ORGANIZATION NAME(S) AND ADDRESS(ES)
NASA Langley Research Center
Hampton, VA 23681-0001

8. PERFORMING ORGANIZATION REPORT NUMBER
L-17203

9. SPONSORING/MONITORING AGENCY NAME(S) AND ADDRESS(ES)
National Aeronautics and Space Administration
Washington, DC 20546-0001

10. SPONSORING/MONITORING AGENCY REPORT NUMBER
NASA TP-3368

11. SUPPLEMENTARY NOTES
Hooker: Clemson University, Clemson, SC; Wise, Carlberg, and Stephens: Langley Research Center, Hampton, VA; Simchick: Lockheed Engineering & Sciences Company, Hampton, VA; Farjami: Christopher Newport University, Newport News, VA.

12a. DISTRIBUTION/AVAILABILITY STATEMENT
Unclassified–Unlimited

Subject Category 76

12b. DISTRIBUTION CODE

13. ABSTRACT *(Maximum 200 words)*

An aging study was performed to determine the stability of $YBa_2Cu_3O_{7-x}$ ceramics in humid environments at 20°C. In this study, fired ceramic specimens were exposed to humidity levels ranging from 30.5 to 100 percent for 2-, 4-, and 6-week time intervals. After storage under these conditions, the specimens were characterized by X-ray diffraction (XRD), scanning electron microscopy (SEM), and electrical resistance measurements. At every storage condition evaluated, the fired ceramics were found to interact with H_2O present in the surrounding environment, resulting in the decomposition of the $YBa_2Cu_3O_{7-x}$ phase. XRD data showed that $BaCO_3$, CuO, and Y_2BaCuO_5 were present after aging and that the peak intensities of these impurity phases increased both with increasing humidity level and with increasing time of exposure. Additionally, SEM analyses of the ceramic microstructures after aging revealed the development of needle-like crystallites along the surface of the test specimens after aging. Furthermore, the superconducting transition temperature T_c was found to decrease both with increasing humidity level and with increasing time of exposure. All the specimens aged at 30.5, 66, and 81 percent relative humidity exhibited superconducting transitions above 80 K, although these values were reduced by the exposure to the test conditions. Conversely, the specimens stored in direct contact with water (100 percent relative humidity) exhibited no superconducting transitions.

14. SUBJECT TERMS
High-temperature superconductivity; Decomposition; Humidity

15. NUMBER OF PAGES
13

16. PRICE CODE
A03

17. SECURITY CLASSIFICATION OF REPORT	18. SECURITY CLASSIFICATION OF THIS PAGE	19. SECURITY CLASSIFICATION OF ABSTRACT	20. LIMITATION OF ABSTRACT
Unclassified	Unclassified		